Vietnam Journal of Science and Technology ***57*** *(5) (2019) 645-656*

doi:10.15625/2525-2518/57/5/13338

MODELING AND SLIDING MODE CONTROL FOR A SINGLE FLEXIBLE MANIPULATOR

Nguyen Quang Hoang*, Ha Anh Son

School of Mechanical Engineering, Hanoi University of Science and Technology, No. 1, Dai Co Viet, Hai Ba Trung, Ha Noi

*Email: *hoang.nguyenquang@hust.edu.vn*

Received: 30 November 2018; Accepted for publication: 29 May 2019

Abstract. Due to material savings and acceleration time reduction, robotic manipulators are designed to be more slender. Therefore, the elasticity of the links should be taken into account in the dynamic study and control design. This paper concerns modeling and control of a single flexible manipulator (SFM). The finite element method (FEM) and Lagrangian equations are exploited to establish the dynamic modeling of SFM. Firstly, the Jacobian matrix is built based on kinematic analysis. Then it is used in construction of a mass matrix for each element. The position and vibration of SFM are controlled by conventional sliding mode controller (CSMC). Its parameters are chosen by linearized equations to guarantee the stability of the system. The numerical simulation is carried out to show the efficiency of the proposed approach.

Keywords: flexible manipulator, finite element method, sliding mode control.

Classification numbers: 5.3.2, 5.3.5, 5.3.7.

1. INTRODUCTION

Over the past 30 years, study on dynamics and control of flexible robot manipulators has attracted much attention of researchers [1-8]. Several authors summarized the studies on flexible robot manipulators [9-16], which have evaluated the development process of flexible manipulators from 1983 to 2016. Through these works we can see that the researches mainly focused on the method of dynamic model building and the method of control for this kind of manipulators. The dynamics of flexible manipulators is often described by partial differential equations. In order to facilitate simulation and control design, these partial differential equations are often transformed into ordinary differential equations [17, 18]. Five methods used to solve this problem include: 1. Lumped parameter method (LPM), 2. Finite difference method (FDM), 3. Assumed mode method, (AMM) [Ritz-Galerkin method], 4. Finite element method (FEM), 5. Rigid finite element method (RFEM), or Multibody system method (MBS).

This paper presents an application of FEM and Lagrangian equation to establish a dynamic model of a flexible manipulator. Based on this model a sliding mode controller is then designed for position and vibration suppression. A novelty of this study is the establishment of the Jacobi matrix for the calculation of kinetic energy of elastic beam elements moving in the plane. Based on this Jacobi matrix, it is easy to calculate the mass matrix of a flexible planar manipulators. In addition, the study proposes a method for choosing parameters of the sliding controller based on linearized equation. The proposed approach has been applied to an SFM. The numerical simulation results show that the flexible motion is suppressed when the joint variable reaches its desired position.

2. MODELING OF A PLANAR FLEXIBLE LINK BY FEM

The kinetic and potential energy play an important role in establishing the dynamic model by Lagrangian equation. This section presents the deriving of mass and stiffness matrices from kinetic and potential energy for a flexible link moving in a plane.

2.1. Kinematic description – Jacobian matrix

In general case of planar motion, let's consider a straight flexible link moving in a plane with respect to the fixed coordinate frame $O_0x_0y_0$. The link is considered slender and has a length of L and mass of m_0. Motion of this link is described by motion of the floating frame Oxy $\mathbf{q}_r = [x_0, y_0, \theta]^T$ – the so-called rigid motion and the small flexible deformation around its straight state. Fig. 1(a) shows a flexible link, fixed frame $O_0x_0y_0$ and floating frame Oxy. Neglecting transverse shear, rotary inertia and gravity, the link is treated as the Euler-Bernoulli beam.

In the FEM formulation, the link is divided into N elements with the same length $l = L/N$, and the same mass $m = m_0/N$. Each element has six degrees of freedom. Let's consider the j^{th} element of the link. Flexible motion of this element is described by displacements of two nodes, which are longitudinal, transverse deflection and slopes at the first and second nodes of the element j^{th}. These displacements are collected in a vector as

$$\mathbf{q}_{j,f} = [u_{3j-2}, u_{3j-1}, u_{3j}, u_{3j+1}, u_{3j+2}, u_{3j+3}]^T, j = \overline{1, N}\,.$$

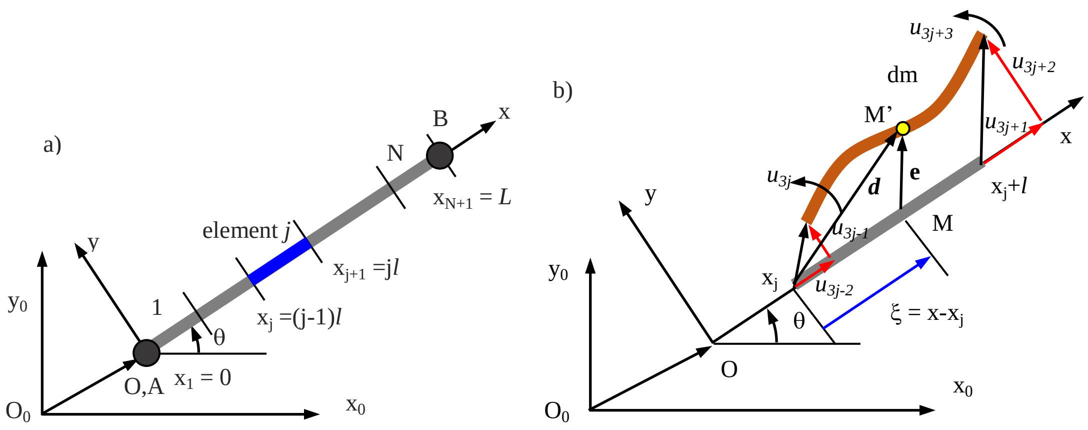

Figure 1. (a) Configuration diagram of a link of manipulator. (b) Typical j^{th} finite element of the link in the floating frame Oxy and the fixed frame $O_0x_0y_0$.

For the whole link, the elastic deformation of the link is described by a vector:

$$\mathbf{q}_f = [u_1, u_2, u_3, \ldots, u_{3N+1}, u_{3N+2}, u_{3N+3}]^T.$$

Motion of j^{th} element and the motion of the link are described by $\mathbf{q}_j = [\mathbf{q}_r^T, \mathbf{q}_{j,f}^T]^T$ and $\mathbf{q} = [\mathbf{q}_r^T, \mathbf{q}_f^{\ T}]^T$, respectively.

Consider a point M belonging to the j^{th} element on the manipulator at a distance $x=x_j+\xi$ from O at undeformable state, when the link deforms, the position of the point M in the floating frame is

$$\mathbf{d} = \mathbf{x} + \mathbf{S}(\xi)\mathbf{q}_{j,f}, \qquad 0 \le \xi \le l, \tag{1}$$

where $\mathbf{x} = [x_j + \xi, 0]^T$ and a matrix $\mathbf{S}$ containing mode shapes as [20, 21]

$$\mathbf{S} = \begin{bmatrix} g_1(\xi) & 0 & 0 & g_2(\xi) & 0 & 0 \\ 0 & h_1(\xi) & h_2(\xi) & 0 & h_3(\xi) & h_4(\xi) \end{bmatrix}$$

with

$$\begin{aligned} g_1 &= (1 - \xi / l),\ g_2 = \xi / l, \\ h_1 &= (2\xi^3 - 3l\xi^2 + l^3) / l^3, \\ h_2 &= (\xi^3 - 2l\xi^2 + l^2\xi) / l^2, \\ h_3 &= (-2\xi^3 + 3l\xi^2) / l^3,\ h_4 = (\xi^3 - l\xi^2) / l^2. \end{aligned}$$

Thus, position of point M’ in the fixed frame with (1) is

$$\mathbf{r} = \mathbf{r}_0 + \mathbf{A}(\theta)\mathbf{d} = \mathbf{r}_0 + \mathbf{A}(\theta)(\mathbf{x} + \mathbf{S}\mathbf{q}_{j,f}), \tag{2}$$

where

$$\mathbf{A}(\theta) = \begin{bmatrix} \cos\theta & -\sin\theta \\ \sin\theta & \cos\theta \end{bmatrix}. \tag{3}$$

is a rotation matrix of the floating frame respect to the fixed frame, and $\mathbf{r}_0 = [x_0 \quad y_0]^T$ is a position vector of the origin O of the floating frame in the fixed frame.

Velocity of the point M is obtained by differentiating (2) with respect to time

$$\dot{\mathbf{r}} = \dot{\mathbf{r}}_0 + \dot{\mathbf{A}}(\theta)(\mathbf{x} + \mathbf{S}\mathbf{q}_{j,f}) + \mathbf{A}(\theta)\mathbf{S}\dot{\mathbf{q}}_{j,f} \tag{4}$$

From (3) we get

$$\dot{\mathbf{A}}(\theta) = \dot{\theta}\begin{bmatrix} -\sin\theta & -\cos\theta \\ \cos\theta & -\sin\theta \end{bmatrix} = \dot{\theta}\mathbf{A}'(\theta)$$

Putting above equation into (4) one obtains

$$\dot{\mathbf{r}} = \dot{\mathbf{r}}_0 + \dot{\theta}\mathbf{A}'(\theta)(\mathbf{x} + \mathbf{S}\mathbf{q}_{j,f}) + \mathbf{A}(\theta)\mathbf{S}\dot{\mathbf{q}}_{j,f} \tag{5}$$

By rearranging the derivative variables, equation (5) becomes

$$\dot{\mathbf{r}} = \mathbf{J}(\mathbf{q}_j)\dot{\mathbf{q}}_j \tag{6}$$

The Jacobian matrix of element j^{th} is determined as:

$$\mathbf{J}(\mathbf{q}_j) = \begin{bmatrix} \mathbf{I}_2 & \mathbf{A}'(\theta)(\mathbf{x} + \mathbf{S}\mathbf{q}_{j,f}) & \mathbf{A}(\theta)\mathbf{S} \end{bmatrix} \tag{7}$$

with $\mathbf{I}_2$ is a 2×2 identity matrix. The matrix $\mathbf{J}(\mathbf{q}_j)$ plays an important role in calculating the mass matrix of the element and the link.

2.2 Kinetic energy and mass matrix

Kinetic energy of j^{th} element of the link is given by:

$$T_j = 0.5\int_e \dot{\mathbf{r}}^T \dot{\mathbf{r}}\, dm$$

with the mass $dm = m_0 l^{-1} d\xi$ and $\dot{\mathbf{r}}$ from (6) one obtains

$$\begin{aligned} T_j &= 0.5\dot{\mathbf{q}}^T \left(m_0 l^{-1} \int_0^l \mathbf{J}^T(\mathbf{q}_j)\mathbf{J}(\mathbf{q}_j) d\xi \right) \dot{\mathbf{q}} \\ &= 0.5\dot{\mathbf{q}}^T \mathbf{M}(\mathbf{q}_j)\dot{\mathbf{q}} \end{aligned} \tag{8}$$

Substituting the Jacobian matrix from (7) into (8), the mass matrix of the j^{th} element is given by

$$\mathbf{M}(\mathbf{q}_j) = \begin{bmatrix} \mathbf{m}_{rr} & \mathbf{m}_{r\theta} & \mathbf{m}_{rf} \\ & \mathbf{m}_{\theta\theta} & \mathbf{m}_{\theta f} \\ sym & & \mathbf{m}_{ff} \end{bmatrix} \tag{9}$$

The elements of mass matrix (9) have following form:

$$\begin{aligned} \mathbf{m}_{rr} &= m_0 l^{-1} \int_0^l \mathbf{I}_2 d\xi, & \mathbf{m}_{rf} &= m_0 l^{-1} \mathbf{A}(\theta) \int_0^l \mathbf{S}\, d\xi, \\ \mathbf{m}_{r\theta} &= m_0 l^{-1} \mathbf{A}'(\theta) \int_0^l \left(\mathbf{x} + \mathbf{S}\mathbf{q}_{j,f} \right) d\xi, & & \\ \mathbf{m}_{\theta\theta} &= m_0 l^{-1} \int_0^l \left(\mathbf{x}^T + \mathbf{q}_{j,f}^T \mathbf{S}^T \right)\left(\mathbf{x} + \mathbf{S}\mathbf{q}_{j,f} \right) d\xi, & & \\ \mathbf{m}_{\theta f} &= m_0 l^{-1} \int_0^l \left(\mathbf{x}^T + \mathbf{q}_{j,f}^T \mathbf{S}^T \right) \mathbf{I}'^T \mathbf{S}\, d\xi, & \mathbf{m}_{ff} &= m_0 l^{-1} \int_0^l \mathbf{S}^T \mathbf{S}\, d\xi \end{aligned}$$

where $\mathbf{I}'^T = \mathbf{A}^T(\theta)\mathbf{A}'(\theta)$.

In case of having concentrated masses at two ends, kinetic energy of these masses must be added. Denote mass and moment of inertia at two ends of the link are m_A, I_A and m_B, I_B. The kinetic energy of the mass at the end A is given by:

$$T_A = 0.5 m_A \dot{r}_A^2 + 0.5 I_A (\dot{\theta} + \dot{u}_3)^2 = 0.5 \dot{\mathbf{q}}_1^T \mathbf{M}_A \dot{\mathbf{q}}_1$$

where $\mathbf{M}_A = m_A \mathbf{J}_{j=1,\xi=0}^T \mathbf{J}_{j=1,\xi=0} + \mathbf{H}_A$ and $\mathbf{H}_A = \partial^2 \left(0.5 I_A \left(\dot{\theta} + \dot{q}_3 \right)^2 \right) / \partial \mathbf{q}_1 \partial \mathbf{q}_1$. Similarly, kinetic energy of the mass at the end B is given by:

$$T_B = 0.5 \dot{\mathbf{q}}_N^T \mathbf{M}_B \dot{\mathbf{q}}_N$$

where $\mathbf{M}_B = m_B \mathbf{J}_{j=N,\xi=l}^T \mathbf{J}_{j=N,\xi=l} + \mathbf{H}_B$ and $\mathbf{H}_B = \partial^2 \left(0.5 I_B \left(\dot{\theta} + \dot{q}_{3N+3} \right)^2 \right) / \partial \mathbf{q}_N \partial \mathbf{q}_N$.

In order to get the mass matrix of the whole link, matrices $\mathbf{Z}_j$ are introduced such that it satisfies the relation $\mathbf{q}_j = \mathbf{Z}_j\mathbf{q}$. Hence, mass matrix of the link has following form:

$$\mathbf{M} = \mathbf{Z}_1^T\mathbf{M}_A\mathbf{Z}_1 + \sum_{j=1}^{N}\mathbf{Z}_j^T\mathbf{M}(\mathbf{q}_j)\mathbf{Z}_j + \mathbf{Z}_N^T\mathbf{M}_B\mathbf{Z}_N \,.$$

2.3. Potential energy and stiffness matrix

Potential energy of the j^{th} element of single link due to elastic deformation is total of strain energy, this is given by [19,20]:

$$\Pi_{j,f} = \frac{1}{2}\int_0^l \left(EA\left(\frac{\partial v}{\partial \xi}\right)^2 + EI\left(\frac{\partial^2 w}{\partial \xi^2}\right)\right) d\xi \,, \tag{10}$$

where v, w is longitudinal and transverse deformation at point M, E is the modulus of elastic and I is the area moment, A is the cross-sectional area. Longitudinal and transverse deformation at point M is given by

$$v = \mathbf{S}_1\mathbf{q}_{j,f}, \qquad w = \mathbf{S}_2\mathbf{q}_{j,f} \tag{11}$$

where $\mathbf{S}_1 = [g_1(\xi) \quad 0 \quad 0 \quad g_1(\xi) \quad 0 \quad 0]$ and $\mathbf{S}_2 = [0 \quad h_1(\xi) \quad h_2(\xi) \quad 0 \quad h_3(\xi) \quad h_4(\xi)]$.

Substituting (11) into (10), one gets

$$\Pi_{j,f} = 0.5\mathbf{q}_{j,f}{}^T \left(\int_0^l \left(EA\mathbf{S}_1^{'T}\mathbf{S}_1^{'} + EI\mathbf{S}_2^{''T}\mathbf{S}_2^{''}\right) d\xi\right)\mathbf{q}_{j,f} = 0.5\mathbf{q}_{j,f}^T\mathbf{K}_{j,f}\mathbf{q}_{j,f} \tag{12}$$

Hence, stiffness matrix of j^{th} element in (12) is determined as:

$$\mathbf{K}_{j,f} = \int_0^l \left(EA\mathbf{S}_1^{'T}\mathbf{S}_1^{'} + EI\mathbf{S}_2^{''T}\mathbf{S}_2^{''}\right) d\xi$$

Together with the rigid coordinates, the stiffness matrix of j^{th} element is given by:

$$\mathbf{K}_j = \begin{bmatrix} \mathbf{0}_{3\times3} & \mathbf{0}_{3\times6} \\ \mathbf{0}_{6\times3} & \mathbf{K}_{j,f} \end{bmatrix}$$

Hence, stiffness matrix of the single link is given by:

$$\mathbf{K} = \sum_{j=1}^{N}\mathbf{Z}_j^T\mathbf{K}_j\mathbf{Z}_j \,.$$

3. DYNAMIC EQUATIONS OF TSFM

The mass and stiffness matrices derived in previous section will be applied to an SFM shown in Fig. 2. This manipulator consists of a slider having mass of m_0, a flexible beam having length L, cross sectional area A, area moment I, made by material with mass density ρ and elastic modulus E, and a payload mass m_t at the left end. The beam is clamped to the slider and driven by a force τ acting on the slider. Motion of the system is defined by motion of the slider $z(t)$ and the flexible deformation $w(x,t)$.

In order to apply FEM for establishing the equation of motion, let's introduce some assumptions: (i) the flexible beam is considered to be an Euler-Bernoulli beam and the longitudinal deformation is neglected; (ii) the gravity effect, actuator dynamics, internal and external disturbances are neglected for simplicity; (iii) the payload is considered as a mass point attached at the right end of the beam.

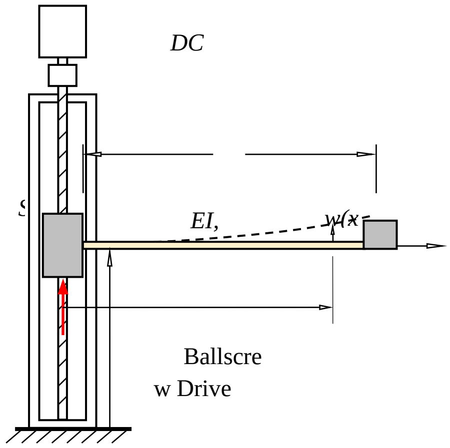

Figure 2. Flexible Cartesian manipulator.

Because the considered link is uniform and has a constant cross section, the number of elements can be chosen as one, $N = 1$. Hence, vector $\mathbf{q}_1$ of the element is

$$\mathbf{q}_1 = [x_0, y_0, \theta, u_1, u_2, u_3, u_4, u_5, u_6]^T .$$

Additionally, longitudinal and transverse deflection and slopes at the first node are zero due to beam be clamped at the left end to the slider, longitudinal deflection of second node also is neglected. Because the w axis and z_0 axis coincide, angular $\theta = 0$ and the slider moves along y-axis, so $x_0 = 0$ and $y_0 = z(t)$. Therefore, the vector of flexible coordinates is given by $\mathbf{q}_f = [u_5, u_6]^T$. The vector of rigid motion coordinates is $\mathbf{q}_r = z$. The whole vector of rigid and flexible coordinates is $\mathbf{q} = [z, u_5, u_6]^T$. Applying the results of the section 2, mass matrix of the flexible system is given by:

$$\mathbf{M} = \begin{bmatrix} \mathbf{m}_{rr} & \mathbf{m}_{rf} \\ \text{sym} & \mathbf{m}_{ff} \end{bmatrix}$$

with $\mathbf{m}_{rr} = \rho AL + m_0 + m_t$,

$$\mathbf{m}_{rf} = \begin{bmatrix} 0.5\rho AL + m_t & -0.5\rho AL^2 \end{bmatrix}, \ \mathbf{m}_{ff} = \begin{bmatrix} \frac{13}{35}\rho AL + m_t & -\frac{11}{210}\rho AL^2 \\ -\frac{11}{210}\rho AL^2 & \frac{1}{105}\rho AL^3 \end{bmatrix}.$$

Stiffness matrix of flexible beam is given by:

$$\mathbf{K} = \begin{bmatrix} 0 & \mathbf{0}_{1\times 2} \\ \mathbf{0}_{2\times 1} & \mathbf{K}_{ff} \end{bmatrix}, \text{ with } \mathbf{K}_{ff} = \frac{EI}{L^3}\begin{bmatrix} 12 & -6L \\ -6L & 4L^2 \end{bmatrix} \tag{13}$$

After having mass and stiffness matrix, under the assumptions, and using Lagrange's equation, the dynamic equation of SFM is obtained by:

$$\begin{bmatrix} \mathbf{m}_{rr} & \mathbf{m}_{rf} \\ \mathbf{m}_{fr} & \mathbf{m}_{ff} \end{bmatrix}\begin{bmatrix} \ddot{\mathbf{q}}_r \\ \ddot{\mathbf{q}}_f \end{bmatrix} + \begin{bmatrix} \mathbf{0} & \mathbf{0}_{1\times 2} \\ \mathbf{0}_{2\times 1} & \mathbf{K}_{ff} \end{bmatrix}\begin{bmatrix} \mathbf{q}_r \\ \mathbf{q}_f \end{bmatrix} = \begin{bmatrix} \boldsymbol{\tau} \\ \mathbf{0}_{2\times 1} \end{bmatrix}. \tag{14}$$

This dynamic equation will be used in designing of a controller and in simulation.

4. CONTROLLER DESIGN

In this section, a robust controller is designed by using sliding mode techniques. The controller is applied for stabilizing vibration at the tip of beam and accuracy position of SFM. The dynamic equation (14) can be decomposed into two sub-systems as:

$$\mathbf{m}_{rr}\ddot{\mathbf{q}}_r + \mathbf{m}_{rf}\ddot{\mathbf{q}}_f = \boldsymbol{\tau}, \tag{15}$$

$$\mathbf{m}_{fr}\ddot{\mathbf{q}}_r + \mathbf{m}_{ff}\ddot{\mathbf{q}}_f + \mathbf{K}_{ff}\mathbf{q}_f = \mathbf{0}. \tag{16}$$

These dynamic equations (15) and (16) will be used to design CSMC. The objective of the controller is to drive the actuated variables $\mathbf{q}_r$ approaching to desire variable $\mathbf{q}_{rd}$, and un-actuated variables $\mathbf{q}_f$ reaching to desired values $\mathbf{q}_{fd}$ asymptotically. In this mathematic model, $\mathbf{q}_{rd}$ is desired position and $\mathbf{q}_{fd}$ is the vibration of tip beam. Objective of controller design is that when $\mathbf{q}_r$ reaches $\mathbf{q}_{rd}$, the flexible motion $\mathbf{q}_{fd}$ converges to zero to eliminate vibration of tip beam. Unactuated dynamics (16) can be rewritten as

$$\ddot{\mathbf{q}}_f = -\mathbf{m}_{ff}^{-1}(\mathbf{m}_{fr}\ddot{\mathbf{q}}_r + \mathbf{K}_{ff}\mathbf{q}_f). \tag{17}$$

Substituting (17) into (15), one obtains the reduced form of system dynamics:

$$\bar{\mathbf{m}}\ddot{\mathbf{q}}_r + \bar{\mathbf{K}}\mathbf{q}_f = \boldsymbol{\tau}, \tag{18}$$

where $\bar{\mathbf{m}} = \mathbf{m}_{rr} - \mathbf{m}_{rf}\mathbf{m}_{ff}^{-1}\mathbf{m}_{fr}$ and $\bar{\mathbf{K}} = -\mathbf{m}_{rf}\mathbf{m}_{ff}^{-1}\mathbf{K}_{ff}$.

From (18), actuated dynamics is modified as:

$$\ddot{\mathbf{q}}_r = \bar{\mathbf{m}}^{-1}(\boldsymbol{\tau} - \bar{\mathbf{K}}\mathbf{q}_f)$$

with $\bar{\mathbf{m}}$ being a positive definite matrix.

Define the errors $\mathbf{e}_r$ and $\mathbf{e}_f$ such that $\mathbf{e}_r = \mathbf{q}_r - \mathbf{q}_{rd}$ and $\mathbf{e}_f = \mathbf{q}_f - \mathbf{q}_{fd} = \mathbf{q}_f$. Thus, the sliding surface is defined by

$$\mathbf{s} = \dot{\mathbf{e}}_r + \boldsymbol{\alpha}\mathbf{e}_r + \boldsymbol{\beta}\mathbf{e}_f = \dot{\mathbf{q}}_r + \boldsymbol{\alpha}\mathbf{e}_r + \boldsymbol{\beta}\mathbf{e}_f \tag{19}$$

In (19), $\boldsymbol{\alpha}$ and $\boldsymbol{\beta}$ are the sliding surface parameters. Derivative of $\mathbf{s}$ with respect to time is determined by

$$\dot{\mathbf{s}} = \ddot{\mathbf{q}}_r + \boldsymbol{\alpha}\dot{\mathbf{q}}_r + \boldsymbol{\beta}\dot{\mathbf{q}}_f \tag{20}$$

when the system states on the sliding surface (19), $\mathbf{s}=0$ so $\dot{\mathbf{s}}=0$, exists and the equivalent control law is applied to the SFM control system.

Considering the case $\dot{\mathbf{s}}=0$, from (20) ones gets $\ddot{\mathbf{q}}_r=-\boldsymbol{\alpha}\dot{\mathbf{q}}_r-\boldsymbol{\beta}\dot{\mathbf{q}}_f$. Then substituting $\ddot{\mathbf{q}}_r$ into (18), the equivalent control is given by

$$\boldsymbol{\tau}_{eq}=\bar{\mathbf{m}}(-\boldsymbol{\alpha}\dot{\mathbf{q}}_r-\boldsymbol{\beta}\dot{\mathbf{q}}_f)+\bar{\mathbf{K}}\mathbf{q}_f \tag{21}$$

The equivalent control (21) can guarantee all state trajectories on the sliding surface (19) when they reach this surface. To verify the system stability, a Lyapunov function candidate is defined as $V=0.5\mathbf{s}^T\mathbf{s}$. The derivative of V with respect to time is defined as $\dot{V}=\mathbf{s}^T\dot{\mathbf{s}}$. To keep these system states on the sliding manifold, we choose $\dot{\mathbf{s}}=-\mathbf{K}\mathbf{s}-\mathbf{k}_n\,\mathrm{sgn}(\mathbf{s})$, with $\mathbf{K}>0$ and

$\mathbf{k}_n>0$. So $\dot{V}=-\mathbf{s}^T\mathbf{K}\mathbf{s}-\mathbf{s}\mathbf{k}_n\,\mathrm{sgn}(\mathbf{s})<0$ when $\mathbf{s}\neq 0$.

with $V>0$, in the sense of Lyapunov, $\dot{V}<0$ should exist to make the SFM system asymptotically stable. As a result, define:

$$\boldsymbol{\tau}_n=\bar{\mathbf{m}}\left(-\mathbf{K}\mathbf{s}-\mathbf{k}_n\,\mathrm{sgn}(\mathbf{s})\right) \tag{22}$$

Finally, the CSMC law of the SFM can be deduced from (21) and (22):

$$\begin{aligned}\boldsymbol{\tau}&=\boldsymbol{\tau}_{eq}+\boldsymbol{\tau}_n\\&=-\bar{\mathbf{m}}\left(\boldsymbol{\alpha}\dot{\mathbf{q}}_r+\boldsymbol{\beta}\dot{\mathbf{q}}_f+\mathbf{K}\mathbf{s}+\mathbf{k}_n\,\mathrm{sgn}(\mathbf{s})\right)+\bar{\mathbf{K}}\mathbf{q}_f\end{aligned} \tag{23}$$

with the CSMC (23), the sliding surface $\mathbf{s}$ converges to zero as time goes to infinity. When $\mathbf{s}=0$ the controller parameters of the CSMC law are selected to make $\lim\mathbf{e}_r=\lim(\mathbf{q}_r-\mathbf{q}_{rd})=0$ as $t\to\infty$, which implies that $\mathbf{q}_r$ converges to $\mathbf{q}_{rd}$. Also, $\lim\mathbf{e}_f=\lim\mathbf{q}_f=0$ as $t\to\infty$, which implies that $\mathbf{q}_f$ converges to zero. Therefore, all the states of the SFM system converge to their desired values as t goes to infinity. Note that the desired values of $\mathbf{q}_f$ are zero. From (17), $\mathbf{s}=0$ and $\dot{\mathbf{s}}=0$, we have the following equations

$$\begin{aligned}\ddot{\mathbf{q}}_f&=-\mathbf{m}_{ff}^{-1}\left(\mathbf{m}_{fr}\ddot{\mathbf{q}}_r+\mathbf{K}_{ff}\mathbf{q}_f\right)\\&=-\mathbf{m}_{ff}^{-1}\left[\mathbf{m}_{fr}\left(-\boldsymbol{\alpha}\dot{\mathbf{q}}_r-\boldsymbol{\beta}\dot{\mathbf{q}}_f\right)+\mathbf{K}_{ff}\mathbf{q}_f\right]\\\dot{\mathbf{e}}_r&=-\boldsymbol{\alpha}\mathbf{e}_r-\boldsymbol{\beta}\mathbf{q}_f\end{aligned} \tag{24}$$

By introducing two variables $\mathbf{z}_1=\mathbf{q}_f$ and $\mathbf{z}_2=\dot{\mathbf{q}}_f$, equations (24) is rewritten as

$$\begin{aligned}\dot{\mathbf{z}}_1&=\mathbf{z}_2\\\dot{\mathbf{z}}_2&=-\mathbf{m}_{ff}^{-1}\left[\mathbf{m}_{fr}\left(-\boldsymbol{\alpha}\left(-\boldsymbol{\alpha}\mathbf{e}_r-\boldsymbol{\beta}\mathbf{z}_1\right)-\boldsymbol{\beta}\mathbf{z}_2\right)+\mathbf{K}_{ff}\mathbf{z}_1\right]\\\dot{\mathbf{e}}_r&=-\boldsymbol{\alpha}\mathbf{e}_r-\boldsymbol{\beta}\mathbf{z}_1.\end{aligned} \tag{25}$$

By rearrangement (25) one obtains

$$\dot{\mathbf{x}}=\mathbf{A}\mathbf{x} \tag{26}$$

where $\mathbf{x}=[\mathbf{z}_1\quad\mathbf{z}_2\quad\mathbf{e}_r]^T$ and

$$\mathbf{A} = \begin{bmatrix} \mathbf{0} & \mathbf{I} & \mathbf{0} \\ -\mathbf{m}_{ff}^{-1}\left(\mathbf{m}_{fr}\boldsymbol{\alpha\beta} + \mathbf{K}_{ff}\right) & \mathbf{m}_{ff}^{-1}\mathbf{m}_{fr}\boldsymbol{\beta} & -\mathbf{m}_{ff}^{-1}\mathbf{m}_{fr}\boldsymbol{\alpha\alpha} \\ -\boldsymbol{\beta} & \mathbf{0} & -\boldsymbol{\alpha} \end{bmatrix}.$$

Matrix **A** in (26) must be a Hurwitz matrix to guarantee the stability of the linearized systems (26). Hence $\mathbf{q}_f, \dot{\mathbf{q}}_f$ converge to zero and $\mathbf{q}_r$ converges to $\mathbf{q}_{rd}$ as t goes to infinity. Therefore, if **A** is Hurwitz matrix then the linear system given by (26) is asymptotically stable [23]. It can be concluded that the CSMC given by (23) when applied to the SFM system guarantees the asymptotic convergence of the states of the system to desired values.

To reduce chattering due to *sgn*(**s**)-function, this function will be replaced by a continuous smooth function as

$$\mathrm{sgn}(\mathbf{s}) \approx 2\pi^{-1}\mathrm{atan}(\gamma\mathbf{s}), \quad \gamma >> 1$$

Now, the control law (23) is modified as

$$\boldsymbol{\tau} = -\bar{\mathbf{m}}\left(\boldsymbol{\alpha}\dot{\mathbf{q}}_r + \boldsymbol{\beta}\dot{\mathbf{q}}_f + \mathbf{K}\mathbf{s} + \mathbf{k}_n 2\pi^{-1}\mathrm{atan}(\gamma\mathbf{s})\right) + \bar{\mathbf{K}}\mathbf{q}_f\,. \tag{27}$$

5. NUMERICAL SIMULATION AND RESULTS

In this section, the dynamic model (15) and (16) are simulated by mean of Matlab to verify the efficiency of the controller design approach. In the simulation, the system parameters of the SFM are set as follows [22]:

$$\begin{aligned} &E = 69\cdot 10^9\,\mathrm{N/\,m^2}, I = 4.1667\cdot 10^{-12}\,\mathrm{m^4}, \\ &\rho = 7850\,\mathrm{kg/\,m^3}, A = 5\cdot 10^{-5}\,\mathrm{m^2}, \\ &L = 0.3\,\mathrm{m}, m_t = 0.01\,\mathrm{kg}, m_0 = 0.455\,\mathrm{kg}. \end{aligned}$$

The dynamics (15) and (16) of SFM is respectively driven by the CSMC input (27). The system parameters of controllers used for simulation are depicted in below. The sliding surface parameters $\boldsymbol{\alpha} = \alpha$, $\boldsymbol{\beta} = [\beta_1, \beta_2]$ also are selected based on the conditions for stability that are obtained by using the Routh-Hurwitz criterion. These conditions guarantee that **A** is a stable matrix. Substituting the system parameters of the SFM into matrix **A**, one gets the conditions

$$\alpha > 0, \quad \beta_2 > 0, \; -4.7\beta_2 > \beta_1 > -33\beta_2\,.$$

Hence, the controller parameters are chosen as

$$\begin{aligned} &\alpha = 6.8, &&\mathbf{K} = 1.2, \quad \mathbf{k}_n = 1.2, \\ &\boldsymbol{\beta} = [-40.8 \quad 3.6], &&\gamma = 50 \end{aligned}$$

In the simulation, the desired state of the SFM is set by vector $\mathbf{q} = [0.3\,\mathrm{m} \quad 0\,\mathrm{m} \quad 0\,\mathrm{rad}]^T$. The simulation results are shown in Figs. 3-6, in which the driving force, motion of the slider and deflection at the right end of beam are presented. From Fig. 4, the slider arrived at the desired position at about 1.35 s. Meanwhile, the controller effectively resists the slender beam oscillations in Fig. 5 and Fig. 6. There is no overshoot in Fig. 4, this indicates that the flexible beam can directly arrive at the desired position instead of moving back and forth around the desired position.

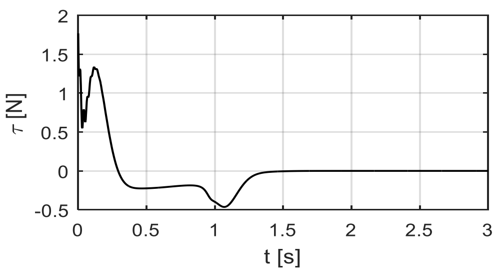

*Figure 3***.** Control force *τ*.

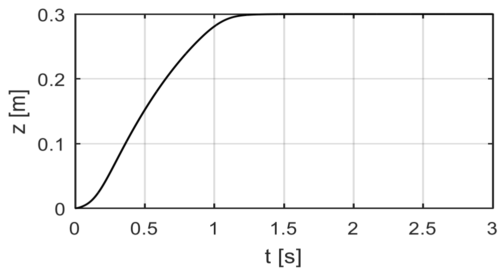

Figure 4. Displacement of slider.

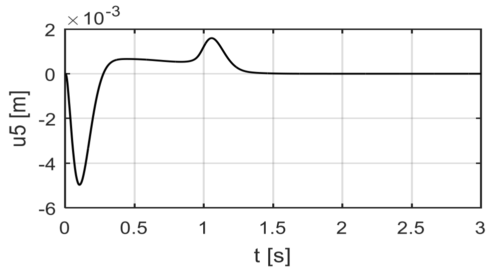

Figure 5. Transverse deflection at the right end of the link.

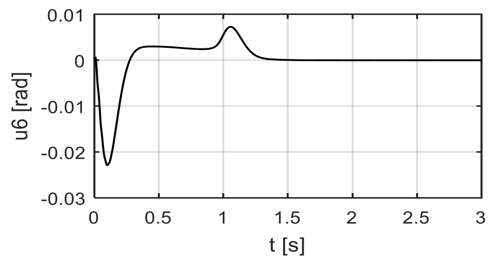

Figure 6. Slope deflection at the right end of the link.

The control force performed by the CSMC law is shown in Fig. 3. In this figure, the driven force jumps back and forth at the outset to suppress the slender beam oscillations. In additionally, the chattering phenomenon is greatly reduced by the smooth function of atan().

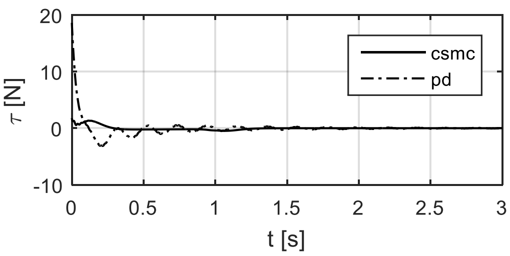

Figure 7. Control force: CSMC vs. PD.

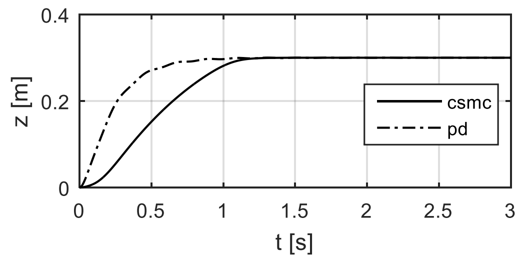

Figure 8. Displacement of Slider: CSMC vs. PD.

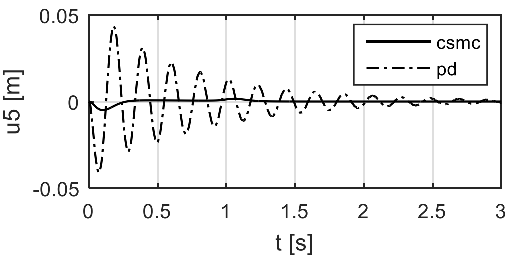

Figure 9. Transverse deflection at the right end of the link: CSMC vs. PD.

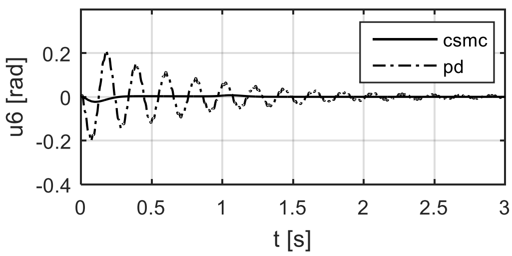

Figure 10. Slope deflection at the right end of the link: CSMC vs. PD.

In order to compare the controller proposed in this paper to another controller, the second simulation is conducted with the traditional PD controller, that is given by

$$\tau_{pd} = -k_p(z - z_d) - k_d\dot{z}, \text{ with } k_p = 62, k_d = 15.$$

The simulation results are shown in Figs.7-10. The results show that with both controllers, the slider is forced to its desired position after about 1.2 second (Fig. 8). Figs. 9 and 10 show that the vibration of the tip mass is suppressed with CSMC better than the one with the PD controller. With the CSMC, the vibration of the tip mass is suppressed after about 1.5 seconds, meanwhile it is more than 3.0 seconds with PD one. In addition, the control force is not smooth as with the CSMC (Fig. 7). These results show the advantages of the CSMC controller in comparison to the traditional PD one.

6. CONCLUSION

In this paper, the mass and stiffness matrices for a flexible link moving in a plane have been established by using a floating frame. Based on these matrices the dynamic equations of a translational flexible link with two masses at two ends are driven. This approach can be extended for any flexible link moving in a plane. By using Jacobian matrix and finite element method, the robot was easily modeled, this method is especially useful for flexible link that has across-sectional change, that flexible link must be divided into many elements. Additionally, the sliding mode controller has been successfully designed for the SFM. The correctness and reliability of the parameter selection method has been confirmed through numerical simulation results.

REFERENCES

1. Ahmed A. Shabana - Flexible Multibody Dynamics: Review of Past and Recent Developments. Multibody System Dynamics **1** (1997) 189–222.
2. Santosha Kumar Dwivedy and Peter Eberhard - Dynamic analysis of flexible manipulators, a literature review. Mechanism and Machine Theory **41** (2006) 749–777.
3. Lochan K., Roy B. K., Subudhi B. - A review on two-link flexible manipulators. Annual Reviews in Control **42** (2016) 346-367.
4. Yanqing Gao, Fei-Yue Wang, Zhi-Quan Zhao - Flexible Manipulators: Modeling, Analysis and Optimum Design, Academic Press, (2012).
5. Valembois R. E., Fisette P., and Samin J. C. - Comparison of Various Techniques for Modelling Flexible Beams in Multibody Dynamics, Nonlinear Dynamics **12** (1997) 367-397.
6. Tamer M. Wasfy and Ahmed K. Noor - Computational strategies for flexible multibody systems, Appl Mech Rev **56** (6) (2003) 533-613.
7. Javier García de Jalón, Eduardo Bayo - Kinematic and Dynamic Simulation of Multibody Systems, The Real-Time Challenge, Springer-Verlag NewYork, Inc., 1994.
8. Esmail Ali Alandoli, Marizan Sulaiman, Rashid M.Z.A., Shah H.N.M, Ismail Z. - A Review Study on Flexible Link Manipulators, Journal of Telecommunication, Electronic and Computer Engineering, ISSN: 2180 – 1843e-ISSN: **8** (2) (2016) 2289-8131.

9. Dwivedy S.K., Eberhard P. (2006): Dynamic analysis of flexible manipulators, a literature review. Mech Mach Theory Article · July 2006 with 321 Re.
10. Chang Tai Kiang, Spowage Chan, Kuan Yoong - Review of Control and Sensor System of Flexible Manipulator, Journal of Intelligent & Robotic Systems **77** (1) (2015) pp 187–213.
11. Hussein, M.T. - A review on vision-based control of flexible manipulators, Journal Advanced Robotics **29** (24) (2015) pp. 1575-1585.
12. Mostafa Sayahkarajy, Z Mohamed, Ahmad Athif Mohd Faudzi - Review of modelling and control of flexible-link manipulators, Proceedings of the Institution of Mechanical Engineers, Part I: Journal of Systems and Control Engineering (2016) 1-13, DOI: 10.1177/0959651816642099.
13. Rahimi H.N. & Nazemizadeh M. - Dynamic analysis and intelligent control techniques for flexible manipulators: a review, Jour. Advanced Robotics **28** (2) (2014) 63-76, DOI: 10.1080/01691864.2013.839079
14. Tokhi M.O., Azad A.K.M. - Flexible Robot Manipulators modeling, simulation and control. The Institution of Engineering and Technology, London, United Kingdom, (2008).
15. Zhi-Cheng Qiu - Adaptive nonlinear vibration control of a Cartesian flexible manipulator driven by a ballscrew mechanism. Mechanical Systems and Signal Processing **30** (2012) pp. 248–266.
16. Benosman, M. and Le Vey, G., Joint trajectory tracking for planar multi-link flexible manipulator: Simulation and experiment for a two-link flexible manipulator. Proceedings of the IEEE International Conference on Robotics and Automation, Washington DC, USA, 11–15 May 2002 (2002) 2461–2466.
17. Thomson W. T., Dahleh M. D. - Theory of Vibration with Applications (5. Ed). Prentice-Hall, Inc., NJ, 2005.
18. Nguyen Van Khang - Engineering vibrations (in Vietnamese). Science and Technics Publishing House, 2005.
19. Dang Viet Cuong, Nguyen Nhat Thang, Nhu Phuong Mai - Strength of material (in Vietnamese). Science and Technical Publishing House, Ha Noi, 2002.
20. Chu Quoc Thang - Finite element method (in Vietnamese). Science and Techn. Publishing House, Ha Noi, 1997.
21. Tran Ich Thinh, Ngo Nhu Khoa - Finite element method (in Vietnamese). Science and Technics. Publishing House, Ha Noi, 2007.
22. Nguyen Quang Hoang, Nguyen Van Quyen - Modeling and Simulation of Translation Single Flexible Manipulator. Proc. of the ICEMA3, 2014.
23. Nguyen Doan Phuoc, Phan Xuan Minh, Han Thanh Trung, Nonlinear control theory (in Vietnamese). Science and Technics Publishing House, Ha Noi, 2003.